

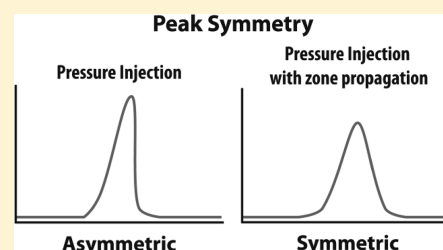
# Peak-Shape Correction to Symmetry for Pressure-Driven Sample Injection in Capillary Electrophoresis

Mirzo Kanoatov, Coraline Retif, Leonid T. Cherney, and Sergey N. Krylov\*

Department of Chemistry and Centre for Research on Biomolecular Interactions, York University, Toronto, Ontario M3J 1P3, Canada

## S Supporting Information

**ABSTRACT:** Pressure-driven sample injection in capillary electrophoresis results in asymmetric peaks due to difference in shapes between the front and the back boundaries of the sample plug. Uneven velocity profile of fluid flow across the capillary gives the front boundary a parabolic shape. The back side, on the other hand, has a flat interface with the electrophoresis run buffer. Here, we propose a simple means of correcting this asymmetry by pressure-driven “propagation” of the injected plug, with the parabolic sample–buffer interface established at the back. We prove experimentally that such a propagation procedure corrects peak asymmetry to the level comparable to injection through electroosmosis. Importantly, the propagation-based correction procedure also solves a problem of transferring the sample into the efficiently cooled zone of the capillary for capillary electrophoresis (CE) instruments with active cooling. The suggested peak correction procedure will find applications in all CE methods that rely on peak shape analysis, e.g., nonequilibrium capillary electrophoresis of equilibrium mixtures.



Capillary electrophoresis (CE) is a powerful platform for a variety of analytical applications, including kinetic studies of biomolecular interactions by kinetic capillary electrophoresis (KCE).<sup>1</sup> In KCE, kinetic constants are extracted from experimental electropherograms by analyzing peak shapes through one of the available approaches. The pattern-based approach to data analysis involves iterative fitting of simulated electropherograms obtained with varying kinetic constants to experimental data through analytical solutions of sample propagation patterns. Some KCE methods also allow the determination of kinetic constants through a simpler parameter-based approach. In the parameter-based approach, a few parameters, such as peak areas and migration times, are first acquired from experimental electropherograms and are then used in simple algebraic expressions to solve for kinetic constants. KCE methods to which parameter-based analysis techniques have been developed include plug–plug KCE,<sup>2</sup> macroscopic approach to studying kinetics at equilibrium (MASKE),<sup>3</sup> and perhaps the most popular of the KCE methods, nonequilibrium capillary electrophoresis of equilibrium mixtures (NECEEM).<sup>4</sup> Both the pattern and parameter-based approaches to KCE data analysis share an assumption that different components of the analyte travel within the capillary in symmetric zones and, thus, result in symmetric electropherogram peaks. In a pattern-based approach, asymmetry in shape of peaks can be mistakenly interpreted by the fitting software as due to interactions between the molecular species. In the parameter-based approach, peak symmetry is relied upon when setting boundaries between merging components of an electropherogram.<sup>5</sup> Thus, deviation from symmetry in electropherogram peaks may significantly affect

the accuracy of both pattern and parameter-based KCE data analysis approaches.

Asymmetry of analyte zones in CE can be caused by both physical processes that occur during electrophoresis and initial asymmetry of the injected sample plug. Physical processes that affect the symmetry of analyte zones include solute adsorption/desorption on/from the capillary walls and dispersive phenomena during electromigration. The importance of the former has been recognized and thoroughly studied.<sup>6–9</sup> The effects of the latter have also been analyzed extensively, using both computer simulations and experiments,<sup>10–12</sup> and can be easily minimized through matching the sample and electrophoresis run buffers.<sup>11,12</sup> Finally, the influence of geometrical factors (such as the capillary edge and the starting zone length) on the zone asymmetry has been investigated.<sup>13,14</sup> In particular, the initial geometric shape of the injected sample plug can have an effect on the symmetry of the resultant electrophoretic peaks. Pressure-driven sample injection into the capillary is used for the majority of practical purposes and, unlike electroosmotic/electrokinetic injection, does not cause electric field-induced injection biases for analytes with different electrophoretic mobilities.<sup>15,16</sup> However, due to the parabolic profile of pressure-driven flow,<sup>17</sup> pressure-injected sample plugs have an asymmetric shape, shown in Figure 1A. The asymmetry of this plug shape is caused by the fact that the posterior side of the sample plug lacks an interface with the electrophoresis run buffer prior to the start of electromigration. This makes the

**Received:** August 19, 2011

**Accepted:** November 27, 2011

**Published:** November 27, 2011

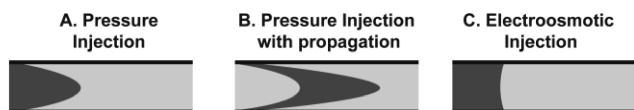


**Figure 1.** Conceptual illustration of initial sample plug shape injected by pressure (A); by pressure, with subsequent pressure-driven sample propagation (B); and by electroosmosis (C).

posterior boundary flat after the electromigration begins, in contrast to the parabolic front boundary (Figure 1A). This asymmetry in the plug shape translates into the asymmetric shape of the resultant peak on the electropherogram.<sup>11,18</sup> Such asymmetry in peaks can be detrimental to accuracy of parameter-based KCE methods. The goal of this work was to study asymmetry of pressure-driven injection into a capillary and to find a way to minimize its adverse effects.

To correct the described asymmetry, we propose to introduce an additional pressure-driven sample propagation step. In such a case, a second pressure pulse is applied after the sample vial is replaced with the electrophoresis run buffer vial. This way, both the front and the back sides of the plug will have the parabolic buffer–sample interfaces (Figure 1B). We hypothesize that this approach will correct the peak shape, making it more symmetric. To assess symmetry improvements, we will compare the shape of the peaks injected by pressure, with and without the propagation step, and by electroosmotic injection. Due to the nature of electroosmotic flow in narrow capillaries, the resultant sample plugs have a nearly rectangular profile (Figure 1C)<sup>16,19</sup> and can thus serve as a reference standard for symmetry.

## RESULTS AND DISCUSSION

A peak is perfectly symmetric if its right and left parts, designated relative to its maximum point, are mirror images of each other. There are various approaches available to describe the symmetry of a peak.<sup>14,20–22</sup> The majority of such approaches are based on the description of peak tailing, a common phenomenon observed in chromatography. For example, the ratio between the back and front half-widths ( $b_{0.1}$  and  $a_{0.1}$ ) at 10% of the peak height or the ratio between the total width  $w_{0.05}$  and twice the front half-width  $f_{0.05}$  at 5% of the peak height are often used to quantitatively characterize the peak symmetry.<sup>20,21</sup> The first is simply termed the peak asymmetry factor,  $A_s$ , while the latter is usually named the tailing factor,  $T_f$ :

$$A_s = b_{0.1}/a_{0.1}, \quad T_f = w_{0.05}/2f_{0.05} \quad (1)$$

Definitions that are based on tailing or fronting describe peak's asymmetry only through parts of its geometry, typically near its baseline. These definitions are also "asymmetric" in nature. Pressure-driven injection, however, creates peaks which are asymmetric around their maximum point without significantly affecting their baseline (Figure 1A). For this reason, fronting/tailing-based definitions of asymmetry are not suitable for characterizing this kind of asymmetry. Instead, for our purpose, we define peak asymmetry through comparing entire areas  $A_{\text{front}}$  and  $A_{\text{tail}}$  of the right and left parts of the peak, respectively (Figure 2). We coin the term of peak asymmetry factor (PAF) for this "symmetric" quantitative characteristic:

$$\text{PAF} = (A_{\text{front}} - A_{\text{tail}})/(A_{\text{front}} + A_{\text{tail}}) \quad (2)$$

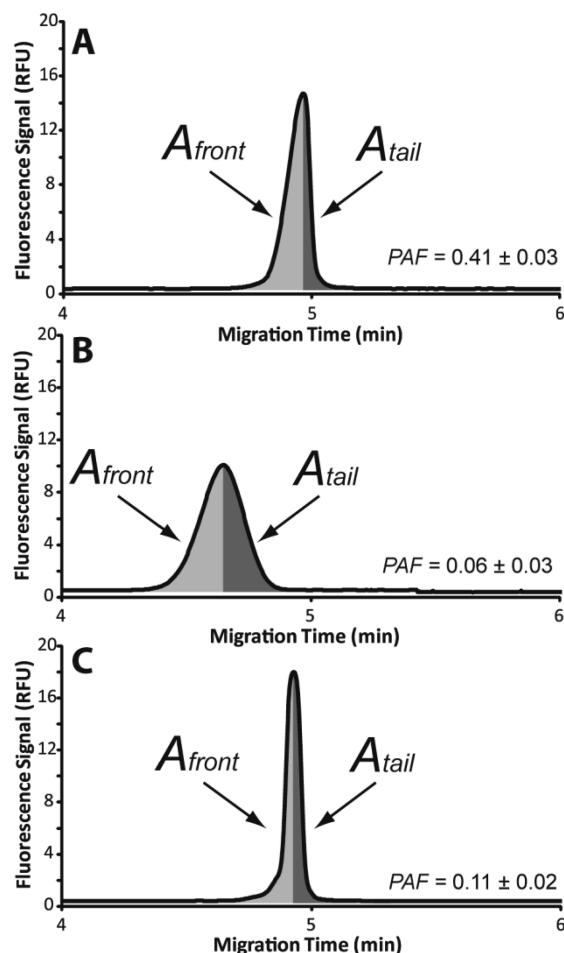


**Figure 2.** Experimental temporal electropherograms of a DNA sample injected through pressure-driven injection (A); pressure-driven injection with subsequent pressure-driven sample zone propagation (B); and electroosmotic injection (C).

Values of PAF range between  $-1$  and  $1$ . The value of  $-1$  corresponds to extreme tailing; the value of  $1$  corresponds to extreme fronting, and the value of  $0$  corresponds to a perfectly symmetric peak.

We have used a fluorescently labeled DNA molecule as an analyte for this study. DNA is negatively charged and does not adsorb onto the inner wall of a bare-silica capillary. This eliminates peak asymmetry that is caused by analyte–capillary surface interactions. After injection, electromigration (the combination of the electroosmotic flow and the electrophoretic force) is used to move the injected plug to the fluorescence detector. To minimize peak asymmetry due to dispersive phenomena during electromigration, the analyte was diluted in 50 mM Tris–acetate at pH 7.5, which was also used as the electrophoresis run buffer.

There are two ways of presenting electropherograms in CE: signal versus migration time in a fixed point in a capillary and signal versus position in a capillary for fixed time. The first way of presentation is more typical as it corresponds to the most common experimental detector design: single-point detector. We will call such an electropherogram "temporal". The signal versus position presentation is not widely used as it requires imaging-type detectors, such as CCD, and capillaries transparent along a large part of their length. Such a setup is not common in CE practice. However, for the purpose of

theoretical consideration, such “spatial” electropherograms can be useful. Temporal and spatial electropherograms are similar, although the front of the peak in the temporal electropherogram appears to the left of the maximum point, while in the spatial electropherograms, it is at the right.

Figure 2A shows the peak shape in a temporal experimental electropherogram for a pressure-injected plug of DNA. The peak displays pronounced fronting; the side corresponding to the shorter migration time is larger in area than the one corresponding to longer times. The calculated PAF was equal to  $0.41 \pm 0.03$ , representing significant asymmetry of the peak. The shape of this peak can be explained purely by the asymmetry of the initial sample plug. To illustrate the point, theoretical spatial electropherograms were generated (Figure

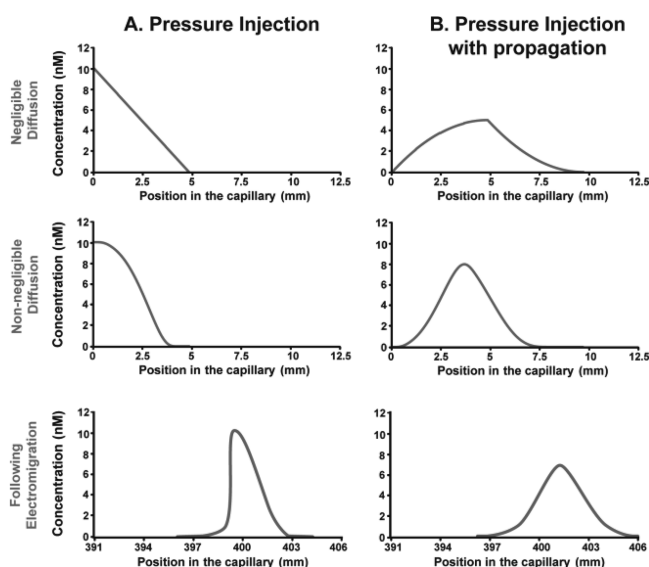


**Figure 3.** Simulated spatial electropherograms of a DNA sample injected through pressure-driven injection (A) and pressure-driven injection with subsequent sample propagation (B). Top row describes concentration profiles of plugs injected with neglect of diffusion. Middle row describes concentration profiles of plugs in cases when diffusion is non-negligible during injection. The bottom row describes concentration profiles of plugs after electromigration to the detector.

3A), using a computational software described previously.<sup>18</sup> The velocity of a pressure-driven flow in a capillary depends on the distance from the capillary walls. It is the highest along the capillary axis, and it is equal to zero at the walls, due to friction. Accordingly, the interface between the run buffer and the sample has a characteristic parabolic shape with the analyte being in the center of the capillary and the buffer being near the walls (Figure 1A). When pressure-driven injection ends, the reservoir with the sample is replaced with one containing the run buffer. The time required for this change is typically sufficient for the complete elimination of the radial concentration gradients by diffusion; therefore, for every cross-section in a capillary, we can define a single concentration of the analyte. It is obvious that (i) such concentration is the smallest in the cross-section drawn through the tip of the parabola and (ii) the concentration grows toward the capillary entrance. If transverse diffusion is negligible, the spatial concentration profile of the analyte within a plug with a parabolic front boundary (Figure 1A) has a characteristic linear shape (Figure 3A, top panel).<sup>17,18</sup> If transverse diffusion is non-negligible, it partially distorts the parabolic interface and makes

this shape nonlinear but still fully asymmetric (Figure 3A, middle panel). After injection, a high voltage is applied across the capillary, and the analyte is moved by electromigration. With properly matched sample and electrophoresis run buffers, electromigration does not significantly alter the shape of the sample plug.<sup>12</sup> Therefore, in the absence of longitudinal diffusion, the analyte distribution shown in Figure 3A, middle panel, would have been maintained. However, longitudinal diffusion cannot be neglected during a relatively long period of electromigration. Thus, as a result of diffusion, the sharp interface at the back of the plug is smoothed out (Figure 3A, bottom panel). The resulting peak shape in this theoretical temporal electropherogram is similar to that observed in the experimental temporal electropherograms shown in Figure 2A.

The degree to which sample plug shape becomes asymmetric depends on the inner diameter of the capillary. Experiments with wider capillary diameters result in more asymmetric peaks (Figure S2, Supporting Information). Two factors contribute to this trend: differences in sample flow velocities and transverse sample diffusion during injection. At a given pressure, maximum flow velocities of a sample will be lower in narrower capillaries. Due to the fact that flow velocity is always equal to zero at the walls of the capillary, milder gradients of flow velocities are established in cross sections of capillaries with smaller diameters. This leads to a less pronounced parabolicity of sample plug boundaries. In addition, the contribution of diffusion during sample injection is more pronounced in narrower capillaries. As the sample is injected into a capillary, transverse diffusion disturbs the parabolic shape of the plug boundary, making it flatter. The time required for a given sample to completely diffuse across the capillary is shorter for capillaries with smaller inner diameters. Taken together with the fact that, at a given pressure, the sample flow velocities are lower, the transverse sample diffusion will smooth out the plug boundary shape to a much greater degree in smaller-diameter capillaries. With the samples used in this study, peak asymmetry due to pressure injection was negligible in a capillary with a 20  $\mu\text{m}$  inner diameter (Figure S2A, Supporting Information). In a 100  $\mu\text{m}$  inner diameter capillary, however, peak asymmetry was so pronounced, that it could have been mistaken for a bimolecular complex decay region in NECEEM measurements (Figure S2B, Supporting Information). While capillaries with smaller inner diameters have better heat dissipation properties, their use is not always preferential. Some application may require large diameter capillaries for better sample detection and larger sample volumes (e.g., in aptamer selection).

These conclusions, regarding the cause of peak asymmetry, suggest a hypothetical method of correcting it by introducing a parabolic sample–buffer interface at the back of the plug. Such an interface can be created by a pressure-driven propagation of the plug after the sample reservoir is replaced with the electrophoresis run buffer. Again, we assume that the time of switching the inlet reservoirs is sufficient for the elimination of radial concentration gradients of the analyte within the capillary by diffusion. Pressure-driven flow with two sample–buffer interfaces will create a parabolic concave boundary at the back and a parabolic convex boundary at the front of the plug. If transverse diffusion is negligible during the injection with pressure-driven propagation, the analyte concentration profile will have the characteristic shape shown in Figure 3B (top panel). If transverse diffusion is not negligible, it will smooth the features of the peak during the injection with propagation (Figure 3B, middle panel). It should be noted that, in both



cases, the improvement in a plug's symmetry occurs as a result of a change in the initial geometric shape of the plug rather than the effects of the Gaussian convolution. Subsequent prolonged electromigration of the sample causes further smoothing of the peak due to the longitudinal diffusion (Figure 3B, bottom panel). It is obvious, even without calculation of PAF, that the pressure-driven propagation step is expected to make the peak more symmetric, although at the expense of some broadening of the sample plug. While peak broadening has adverse effects on the separation power of CE, the degree of this broadening can be controlled by the distance of sample propagation.

To confirm our hypothesis, experiments that included pressure-driven sample propagation were performed. After the injection of the sample plug, it was further propagated by a longer pulse of lower pressure 5 cm along the capillary. (This particular propagation distance was chosen to avoid overheating the sample in the inefficiently cooled region of the capillary, which has a length of approximately 4 cm. Most instruments with active cooling systems do not cool the entire length of the capillary to an equal degree. It has been shown that sample heating in inefficiently cooled areas of the capillary can be significant and may affect molecular interactions under study.<sup>23</sup> In all commercial instruments with active cooling, the inlet of the capillary is inefficiently cooled. Thus, pressure-driven propagation of the analyte through this region helps to avoid sample overheating.) A fragment of the resulting experimental temporal electropherogram is shown in Figure 2B. The peak is more symmetric than the one obtained without the propagation step (Figure 2A), with PAF value equal to  $0.06 \pm 0.03$ . Similar effects were also observed in a capillary with a greater inner diameter (Figure S2C, Supporting Information) and also when fluorescein, a small molecule with a greater diffusion coefficient, was used as an analyte (Figure S1, Supporting Information). Experimental results also confirmed that peak broadening occurs during sample propagation. The width of the DNA peak increased from 13 to 28 s after the symmetry correction. Such broadening is typically undesirable but is not detrimental to most KCE experiments as molecular species in KCE are typically separated from each other by minutes.<sup>1–4</sup> Peak broadening upon symmetry correction may become a problem if the sample resolution is poor. Also, peak broadening can be more or less significant than the one reported here depending on the sample's density, viscosity, etc. Thus, it is expected that KCE practitioners will perform individual preliminary resolution tests first to determine if the trade-off between the measurement accuracy and sample resolution is warranted for their particular case.

To better gauge the presented PAF values, a meaningful point of reference is required. To provide such a reference point, we measured the PAF value of a peak that results from electroosmotic injection. This injection method is known to produce plugs of nearly perfect symmetry<sup>24</sup> and can, thus, be used as a standard. As seen in Figure 2C, electroosmotic sample injection results in a sharp symmetric peak. The PAF value for this injection was determined to be  $0.11 \pm 0.02$ . The fact that the PAF values for pressure-driven propagation method and electroosmotic injection are within 2 standard deviations of each other suggests that the proposed method does achieve its goal.

All KCE methods are based on a theory that assumes longitudinal symmetry in distribution of interacting components in the initial plug. Thus, the observed asymmetry due to pressure-driven sample injection will affect the accuracy of the

extracted information. Indeed, the application of any KCE method to asymmetric plugs will result in an error in the modeling of initial conditions used in this KCE method. Such an error introduced at the very first step of data analysis will lead to an equal or greater error in final results produced by the KCE method. As shown in Figure 4, the symmetrization of the

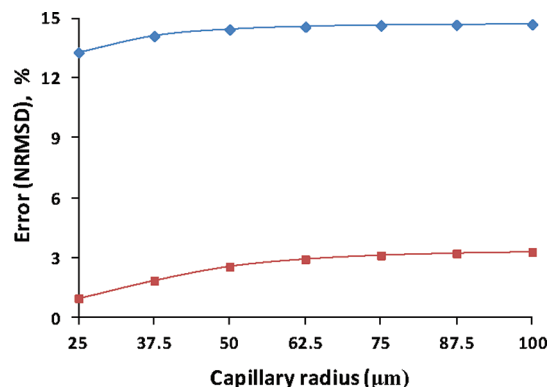


**Figure 4.** Error (NRMSD) for fitting Gaussian peak into the initial peak produced by the pressure-driven injection vs the capillary radius without symmetry correction (blue line) and after symmetry correction (red line).

pressure-driven plugs results in as much as a 5-fold reduction in this initial error. By definition, the error is calculated here as normalized root mean square deviation (NRMSD) using the following expressions:<sup>25,26</sup>

$$\text{NRMSD} = \frac{\sqrt{E(C - G)^2}}{\max C},$$
$$E(C - G)^2 = \frac{1}{N} \sum_{i=1}^N (C_i - G_i)^2 \quad (3)$$

where  $E(C - G)^2$  is the mean square error for the best fit of the Gaussian distribution of concentration,  $G$ , into the DNA concentration profile,  $C$ , in the pressure-driven zone of DNA, and  $N$  is the total number of points in which values  $C_i$  of  $C$  were calculated for simulated peaks (or measured for experimental peaks). By definition, the best fit minimizes the NRMSD value under an additional condition that requires that the Gaussian peak area be equal to the pressure-driven peak area (i.e., total amounts of DNA in peaks are the same). We compared pressure-driven peaks to Gaussian peaks since KCE methods are usually based on the assumption of Gaussian distributions of components in the initial plug. Distributions of DNA in the initial pressure-driven plugs were simulated using previously developed software.<sup>27,28</sup> Examples of fitting Gaussian peaks into initial pressure-driven peaks are shown in Figure S3, Supporting Information. This figure clearly demonstrates that the developed procedure of peak symmetrization allows one to produce initial peaks with a shape that is very close to the Gaussian one. This conclusion is also confirmed by fitting the Gaussian peaks into experimental pressure-driven peaks observed with a fluorescence detector placed at the capillary end (see Figure S4, Supporting Information).

## CONCLUDING REMARKS

Pressure-driven propagation of sample through the capillary can correct the asymmetry of the peak shape, to a level comparable

to that of the electroosmotic injection. The degree to which plug shape becomes asymmetric as a result of pressure injection depends on the inner diameter of the capillary and the diffusion coefficients of the analytes. Besides symmetry correction, pressure-driven sample propagation also causes peak broadening and should, thus, be used with caution when separating multiple species with similar electrophoretic mobilities as peak widening may affect the resolving power of the method. While the observed degree of peak broadening should be acceptable for most KCE-based experiments, its detrimental effects may outweigh the benefits of peak symmetrization in applications with poor resolution of the analytes. Software is available to calculate optimum parameters of sample propagation in order to minimize peak broadening.<sup>18</sup> As a general rule, symmetry can be achieved by making the propagation distance equal to the length of the original sample plug. This ensures that the shape of the parabolic profile at the back of the plug is similar to the initial parabolic shape at the front of the plug. In some applications, however, propagation distance may exceed the length of the original plug: for example, when pressure-driven sample propagation is used to avoid sample overheating. In the experiments described above, the pressure-driven propagation was purposefully made longer than the length of the original plug to achieve this goal. The proposed method should only be used to correct the asymmetry of the plug shape that is due to pressure-driven injection of the sample; asymmetry that results from electrodispersion phenomena or sample adsorption to capillary walls should be addressed as described elsewhere.<sup>6,9,11,12</sup>

## MATERIALS AND METHODS

All chemicals were purchased from Sigma-Aldrich (Oakville, ON, Canada) unless otherwise stated. Fused-silica capillaries were purchased from Polymicro (Phoenix, AZ). DNA sequence was custom synthesized by Integrated DNA Technologies (Coralville, IA). The nucleotide sequence of the fluorescently labeled, single-stranded DNA sequence was 5'-FAM-CTC CTC TGA CTG TAA CCA CG CCG AAG ACC TTT TTA GCG TAC TGA AAA GGA GTT ACT CTC GCA TAG GTA GTC CAG AAG CC-3'. Both the DNA and the fluorescein samples were diluted to 20 nM in 50 mM Tris-acetate at pH 7.5, which was also the electrophoresis run buffer.

All capillary electrophoresis (CE) procedures were performed using a P/ACE MDQ apparatus (Beckman Coulter, Mississauga, ON, Canada) equipped with a laser-induced fluorescence (LIF) detection system. Uncoated fused-silica capillaries with inner diameters of 20, 75, and 100  $\mu\text{m}$  and an outer diameter of 360  $\mu\text{m}$  were used. Runs were performed in 50 cm long (40 cm to the detection window) capillaries. Both the inlet and the outlet reservoirs contained the electrophoresis run buffer (50 mM Tris-acetate at pH 7.5). Prior to every run, the capillaries were rinsed with the run buffer solution. At the end of each run, the capillaries were rinsed with 100 mM HCl, 100 mM NaOH, and deionized water. For pressure injection, the samples were injected into the capillaries prefilled with the run buffer by a pressure pulse of 0.5 psi. The duration of pressure pulses for 20, 75, and 100  $\mu\text{m}$  inner diameter capillaries were 87, 6.2, and 3.5 s, respectively. In each case, the length of the sample plug was calculated to be approximately 7 mm. For experiments with zone propagation, pressure pulses of 0.3 psi were applied for 73 and 41 s after the injection step, for 75 and 100  $\mu\text{m}$  inner-diameter capillaries, respectively. It was calculated that, during this propagation step, the sample plugs

moved 5 cm along the capillary. Electroosmotic injection was carried out by applying an electric potential of 10 kV for 13.5 s across the length of the capillary for a 75  $\mu\text{m}$  inner diameter capillary. Positive electrode was at the inlet side of the capillary. The length of the sample plug for electrokinetic injection was calculated to be 7 mm. Electrophoresis was carried out with the positive electrode at the injection end of the capillary; the direction of the electroosmotic flow was from the inlet to the outlet reservoir. Separation was carried out by an electric field of 500 V/cm. The temperature in the cooled region of the capillary was maintained at 15  $^{\circ}\text{C}$  during the separation.

Upon elution of the DNA sample from the capillary, electropherogram charts were analyzed. Areas from the DNA-corresponding peak were calculated, and PAF was determined using eq 2. Each measurement was replicated 6 times. The average values are presented with one standard deviation as the error.

## ASSOCIATED CONTENT

### Supporting Information

Additional information as noted in text. This material is available free of charge via the Internet at <http://pubs.acs.org>.

## AUTHOR INFORMATION

### Corresponding Author

\*E-mail: [skrylov@yorku.ca](mailto:skrylov@yorku.ca).

## ACKNOWLEDGMENTS

This work was funded by the Natural Sciences and Engineering Research Council of Canada.

## REFERENCES

- (1) Petrov, A.; Okhonin, V.; Berezovski, M.; Krylov, S. N. *J. Am. Chem. Soc.* **2005**, *127*, 17104–17110.
- (2) Okhonin, V.; Petrov, A. P.; Berezovski, M.; Krylov, S. N. *Anal. Chem.* **2006**, *78*, 4803–4810.
- (3) Krylov, S. N.; Okhonin, V.; Berezovski, M. V. *J. Am. Chem. Soc.* **2010**, *132*, 7062–7068.
- (4) Krylov, S. N. *J. Biomol. Screening* **2006**, *11*, 115–122.
- (5) Cherney, L. T.; Kanoatov, M.; Krylov, S. N. *Anal. Chem.* **2011**, *83*, 8617–8622.
- (6) Schure, M. R.; Lenhoff, A. M. *Anal. Chem.* **1993**, *65*, 3024–3037.
- (7) Gas, B.; Stedry, M.; Rizzi, A.; Kenndler, E. *Electrophoresis* **1995**, *16*, 958–967.
- (8) Shariff, K.; Ghosal, S. *Anal. Chim. Acta* **2004**, *507*, 87–93.
- (9) Rodriguez, I.; Li, S. F. Y. *Anal. Chim. Acta* **1999**, *383*, 1–26.
- (10) Reijenga, J. C.; Kenndler, E. *J. Chromatogr., A* **1994**, *659*, 417–426.
- (11) Gas, B.; Kenndler, E. *Electrophoresis* **2000**, *21*, 3888–3897.
- (12) Gebauer, P.; Bocek, P. *Anal. Chem.* **1997**, *69*, 1557–1563.
- (13) Cohen, N.; Grushka, E. *J. Chromatogr., A* **1994**, *684*, 323–328.
- (14) Radko, S. P.; Chrambach, A.; Weiss, G. H. *J. Chromatogr., A* **1998**, *817*, 253–262.
- (15) Huang, X.; Gordon, M. J.; Zare, R. N. *Anal. Chem.* **1988**, *60*, 375–377.
- (16) Krivacsy, Z.; Gelencser, A.; Hlavay, J.; Kiss, G.; Sarvari, Z. *J. Chromatogr., A* **1999**, *834*, 21–44.
- (17) Peng, X. J.; Chen, D. D. Y. *J. Chromatogr., A* **1997**, *767*, 205–216.
- (18) Wong, E.; Okhonin, V.; Berezovski, M. V.; Nozaki, T.; Waldmann, H.; Alexandrov, K.; Krylov, S. N. *J. Am. Chem. Soc.* **2008**, *130*, 11862–11863.
- (19) Tsuda, T.; Ikeda, M.; Jones, G.; Dadoo, R.; Zare, R. N. *J. Chromatogr.* **1993**, *632*, 201–207.
- (20) Piette, V.; Parmentier, F. *J. Chromatogr., A* **2002**, *979*, 345–352.

- (21) Duchemin, V.; Le Potier, I.; Troubat, C.; Ferrier, D.; Taverna, M. *Biomed. Chromatogr.* **2002**, *16*, 127–133.
- (22) Sun, Y.; Kwok, Y. C.; Nguyen, N. T. *Microfluid. Nanofluid.* **2007**, *3*, 323–332.
- (23) Krylov, S. N.; Musheev, M. U.; Filiptsev, Y. *Anal. Chem.* **2010**, *82*, 8692–8695.
- (24) Patankar, N. A.; Hu, H. H. *Anal. Chem.* **1998**, *70*, 1870–1881.
- (25) Lehmann, E. L.; Casella, G. *Theory of point estimation*; Springer: New York, 1998; pp 589.
- (26) DeGroot, M. H.; Schervish, M. J. *Probability and statistics*, 3d ed.; Addison-Wesley, 2002; pp 816.
- (27) Okhonin, V.; Wong, E.; Krylov, S. N. *Anal. Chem.* **2008**, *80*, 7482–7486.
- (28) Krylova, S. M.; Okhonin, V.; Krylov, S. N. *J. Sep. Sci.* **2009**, *32*, 742–756.

## SUPPORTING INFORMATION

### Peak-Shape Correction to Symmetry for Pressure-Driven Sample Injection in Capillary Electrophoresis

Mirzo Kanoatov, Coraline Retif, Leonid T. Cherney, and Sergey N. Krylov\*

Department of Chemistry and Centre for Research on Biomolecular Interactions, York University, Toronto, Ontario M3J 1P3, Canada

#### Experiments with a fluorescein sample

In addition to experiments performed with the DNA sample, similar experiments were also performed with a fluorescein sample. Fluorescein is a negatively charged small molecule. Due to its smaller molecular size, fluorescein possessed a faster diffusion coefficient than the DNA sequence used in this study. Similar to DNA, it does not interact with the walls of a bare-silica capillary, due to its charge. Peak shape of a fluorescein sample should thus not be distorted due to its interactions with the capillary wall.

A sample of 20 nM fluorescein was prepared in 50 mM Tris-Acetate buffer at pH 7.5, and analyzed through capillary electrophoresis. Experiments were performed as described in the main article. First, fluorescein was injected with pressure injection. This resulted in a peak with pronounced fronting (**Fig. S1A**). *PAF* was measured to be  $0.34 \pm 0.08$ . The same sample was then injected with pressure-driven injection with subsequent pressure propagation of the sample by 5 cm along the capillary. This resulted in a somewhat broader, but much more symmetric peak (**Fig. S1B**). *PAF* for this peak was determined to be  $0.04 \pm 0.03$ . To assess the extent of plug shape distortion during electromigration, the same fluorescein sample was injected into the capillary through electroosmosis. This resulted in a sharp symmetric peak (**Fig. S1C**), with *PAF* value equal to  $0.05 \pm 0.03$ . These experiments confirmed that pressure-driven sample propagation also corrects the peak shape of samples with a faster diffusion coefficient.

#### Experiments with capillaries of varying inner diameters

To illustrate the dependence of peak asymmetry caused by pressure-driven injection on the inner diameter of a capillary, experiments with 20 and 100

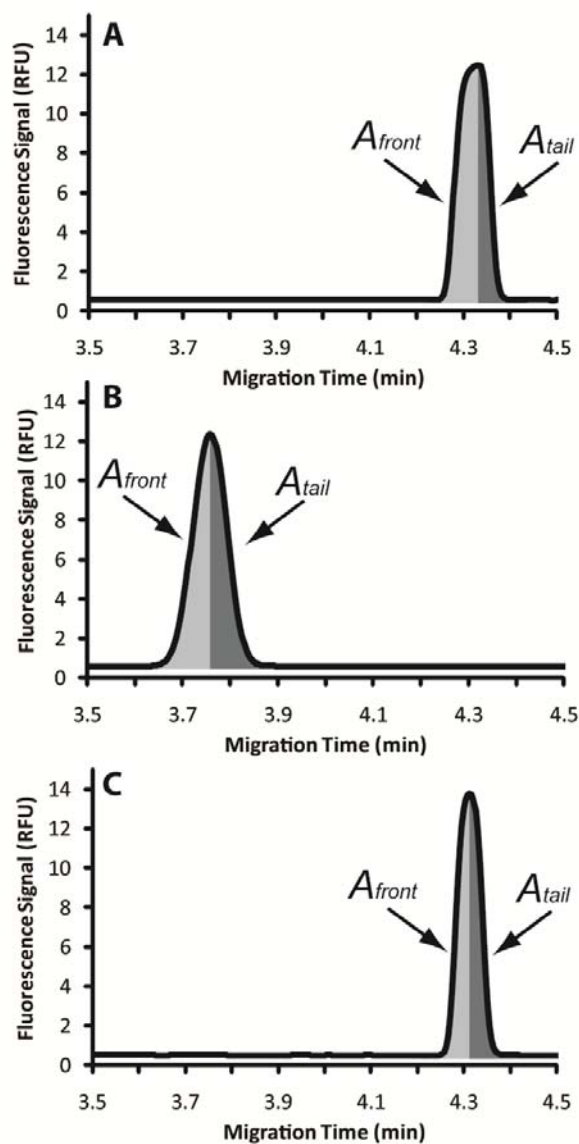


**Figure S1.** Experimental temporal electropherograms of a fluorescein sample injected through pressure-driven injection (A); pressure-driven injection with subsequent pressure-driven sample zone propagation (B); and electroosmotic injection (C).

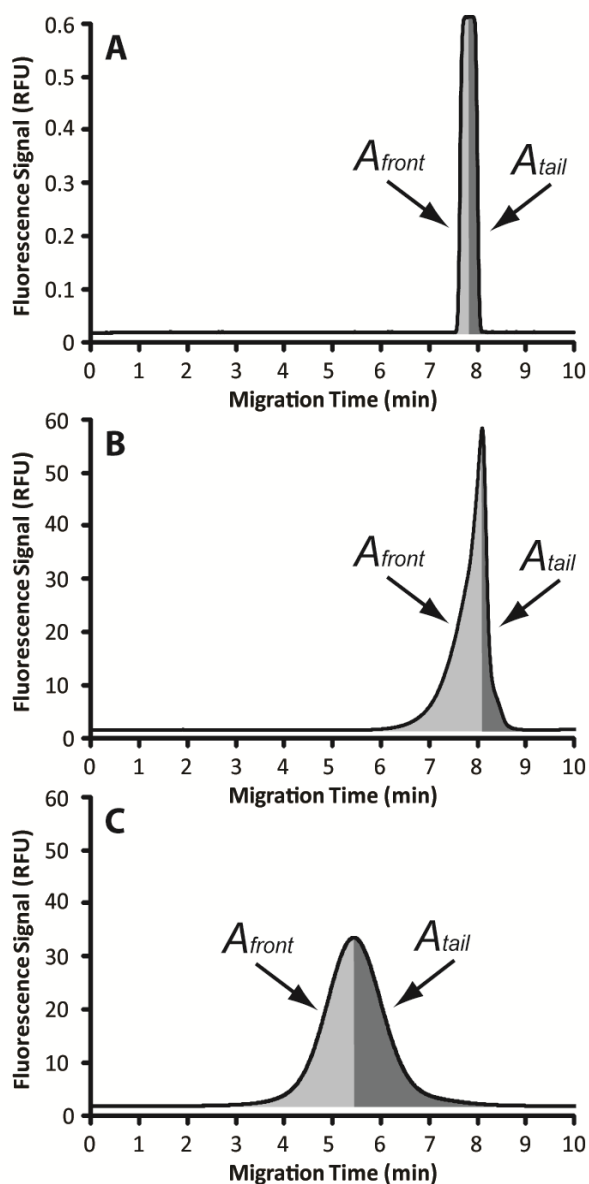


**Figure S2.** Experimental temporal electropherograms of a DNA sample injected through pressure-driven injection into a 20  $\mu\text{m}$  inner diameter capillary (A); 100  $\mu\text{m}$  inner diameter capillary (B); and into a 100  $\mu\text{m}$  inner diameter capillary with subsequent pressure-driven sample zone

symmetry correction are shown in **Fig. S3** by blue lines. The corresponded (best fitted) Gaussian peaks are depicted by red lines. Errors (NRMSD) in fitting Gaussian peaks into the pressure-driven peaks without and with symmetry correction were 13% and 2%, respectively. Thus, the pressure-driven injection with symmetry correction gives 6-fold decrease in the error and allows one to generate practically the Gaussian distribution of solvents in initial plugs.

$\mu\text{m}$  inner diameter capillaries were performed. In both cases, a DNA sample was injected into the capillary by a pressure pulse of 0.5 psi, to match experiments with 75  $\mu\text{m}$  inner diameter capillaries. The duration of the pressure pulse was varied between different capillaries to inject 7 mm-long plugs in both cases. In a 20  $\mu\text{m}$  inner diameter capillary, pressure injected plugs resulted in a sharp symmetric peaks with a flat top (**Fig. S2A**). *PAF* was calculated to be  $0.01 \pm 0.005$ . This peak is essentially symmetric and symmetry correction should not be applied to it as such a correction will only cause peak broadening. In the case of a 100  $\mu\text{m}$  inner diameter capillary, pressure injected plugs resulted in a peak with pronounced fronting (**Fig. S2B**), with a *PAF* value of  $0.53 \pm 0.02$ . Introduction of the pressure-driven propagation step after sample injection significantly improved symmetry of the resultant peaks (**Fig. S2C**), decreasing the *PAF* value to  $-0.01 \pm 0.002$ .

### Best fit of the Gaussian peaks into the pressure-driven peaks

To quantitatively estimate results of symmetry correction for peaks produced by the pressure-driven injection we performed more than 20 simulations of such injection using previously developed software.<sup>1,2</sup> We then modeled each simulated pressure-driven peak by fitting the Gaussian peak (named the best fit) into it. The height, width, and position of the Gaussian peak were varied till an error in fitting reached the minimum. To quantify such an error, we used Normalized Root Mean Square Deviation (NRMSD) defined by expression (3) in the main text. The fitting procedure was performed under an additional constrain that requires that the area of Gaussian peak be equal to that of the corresponding pressure-driven peak. Physically, this condition means that total amounts of DNA in both peaks are the same. Two examples of simulated pressure-driven peaks without and with the



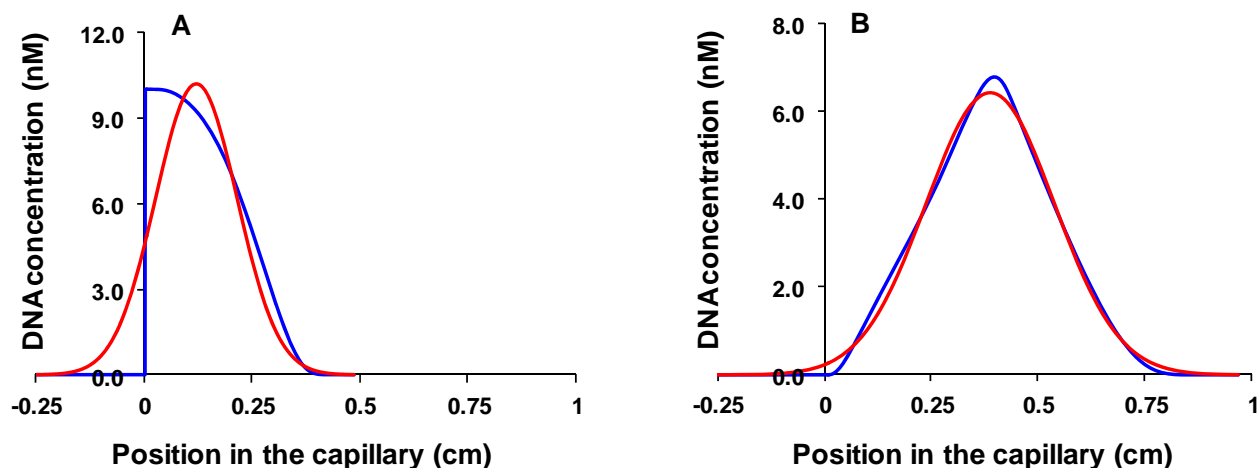


**Figure S3.** The best fit of Gaussian peaks (red lines) into simulated peaks produced by the pressure-driven injection (blue lines) without symmetry correction (**A**) and with symmetry correction (**B**). The area of each Gaussian peak is equal to the area of the corresponding pressure-driven peak.

It should be noted, that longitudinal diffusion leads to a decrease in deviation of the observed peak shape from the ideal Gaussian shape during electromigration stage of CE. **Figure S4** demonstrates two experimental peaks depicted by blue lines. These peaks were observed at the capillary end after the pressure-driven injection (at the capillary beginning) followed by electromigration. The left and right panels in **Fig. S4** correspond to the injection without and with symmetry correction, respectively. The Gaussian peaks obtained by the best fit procedure described above are shown by red lines. Errors (NRMSD) in fitting Gaussian peaks into the pressure-driven peaks generated without and with symmetry correction were 4% and 1%, respectively. Both errors are relatively small though the symmetry correction still gives 4-fold decrease in the error. However, the symmetry improvement due to the longitudinal diffusion during electromigration does not guarantee the successful application of KCE methods. Indeed, the latter relies on the generation of the Gaussian peaks at the capillary beginning (which is a goal of the present study) rather than on having the Gaussian peaks at the capillary end.

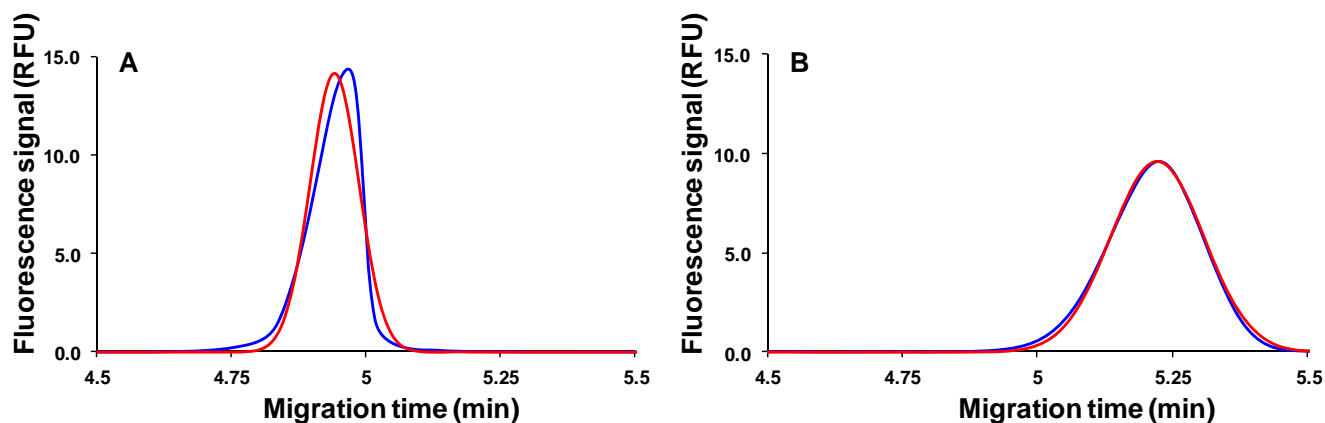


**Figure S4.** The best fit of Gaussian peaks (red lines) into experimental peaks produced by the pressure-driven injection (blue lines) without symmetry correction (**A**) and with symmetry correction (**B**). The area of each Gaussian peak is equal to the area of the corresponding pressure-driven peak.

## REFERENCES

- (1) Okhonin, V.; Wong, E.; Krylov, S. N. *Anal. Chem.* **2008**, 77, 7482 – 7486.
- (2) Krylova, S.M.; Okhonin, V.; Krylov, S.N. *J. Sep. Sci.* **2009**, 32, 742-756.